

## DUAL-AXIS TEST RIG FOR MEMS TILT SENSORS

**Sergiusz Łuczak**

*Warsaw University of Technology, Faculty of Mechatronics, Institute of Micromechanics and Photonics, Division of Design of Precision Devices, Boboli 8, 02-525 Warsaw, Poland (✉ s.luczak@mchtr.pw.edu.pl, +48 22 234 8315)*

### Abstract

The paper addresses the problem of experimental studies of miniature tilt sensors based on low-range accelerometers belonging to Microelectromechanical Systems (MEMS). A custom computer controlled test rig is proposed, whose kinematics allows an arbitrary tilt angle to be applied (i.e. its two components: pitch and roll over the full angular range). The related geometrical relationships are presented along with the respective uncertainties resulting from their application. Metrological features of the test rig are carefully evaluated and briefly discussed. Accuracy of the test rig is expressed in terms of the respective uncertainties, as recommended by ISO; its scope of application as well as the related limitations are indicated. Even though the test rig is mostly composed of standard devices, like rotation stages and incremental angle encoder, its performance can be compared with specialized certified machines that are very expensive. Exemplary results of experimental studies of MEMS accelerometers realized by means of the test rig are presented and briefly discussed. Few ways of improving performance of the test rig are proposed.

Keywords: tilt sensor, accelerometer, MEMS, uncertainty of measurement, test rig.

© 2014 Polish Academy of Sciences. All rights reserved

### 1. Introduction

While surveying papers devoted to tilt sensors built of low-range MEMS accelerometers, it is easy to find out that problems connected with the related experimental studies are often not given enough attention. The aim of the paper is to bridge this gap.

The experimental works are necessary especially when metrological parameters of the accelerometers are of a high importance, mainly in the case when:

- significant metrological parameters of a sensor are not provided (e.g. prototype sensor, like the one described in [1]),
- values of important metrological parameters of a sensor are over- or under-estimated in the related catalog,
- a sensor must be calibrated by the user (there exist also some calibration methods with no test rig necessary, described e.g. in [2, 3], however their application results in a decrease of the accuracy of the sensor calibrated that way),
- results of ageing of a sensor must be determined.

Notwithstanding many advantages of MEMS sensors, like low cost, low power consumption, small dimensions and high resistance to mechanical shock, their main shortcoming still remain poor metrological parameters, much worse compare to their conventional counterparts. Such situation provides an opportunity for many researchers and designers, who strive for improvement of the performance of the MEMS devices by performing appropriate experiments, where two crucial issues are methodology of their realization and the related test rig, whose precision significantly influences

the results to be obtained.

One of the most frequent applications of low-range MEMS accelerometers are tilt measurements, despite the fact that their accuracy is relatively low. In order to carry out experimental studies of a respective tilt sensor built of MEMS accelerometers, there are four options possible:

- applying special certified machines used e.g. in [4] (very expensive option),
- applying an adapted universal test rig, e.g. a standard equipment like a theodolite used in [2] or a three-way milling vise used in [5] (featuring usually a manual drive),
- integrating standard devices like rotation stages or inclinometers referred to in [6–9] (most commonly accepted option),
- constructing a custom test rig, like the one in [10] (most seldom option).

As long as a complete equipment is used, there is usually nothing to question. However, if the test rig is integrated using some standard components, the researchers often have not paid enough attention to the employed test rig and the applied methodology, as it is the case e.g. in [6–9], where the result were overestimated errors of the tested sensors, e.g. hysteresis evaluated by Ang et al in [8], being rather the hysteresis of the employed test rig itself. Authors usually provide only information on the angular resolution of applying tilt angles without any evaluation of the related accuracy, not mentioning the problem of aligning the rotation axes of the test rig with respect to the gravity vector and to each other.

Therefore, it was considered purposeful to present a detailed description of a test rig that is relatively inexpensive, yet provides satisfactory performance with regard to low-range MEMS accelerometers. Taking into account catalog data pertaining to operation of these sensors, it was assumed that the test rig must meet the following basic technical requirements:

- applying angular position of the tested sensor over  $360^\circ$  around two perpendicular axes with accuracy of  $0.02^\circ$ ,
- measuring analog output voltages of the tested sensor with accuracy of 0.005 V,
- recording the applied angular positions of the tested sensors with its corresponding indications in computer memory,
- performing automatically series of measurements over a pre-defined angular range.

The accepted values of the accuracies result from accuracy of the MEMS sensors to be tested, evaluated on the basis of the data reported in respective catalogs (assuming that the accuracy of the measuring instrument should be at least 10 times higher than the accuracy of the measured quantity).

## 2. Geometrical relationships

It is commonly accepted that tilt is represented by two components: pitch and roll [11]. Therefore, the test rig should make it possible to apply pitch and roll directly. Fig. 1 illustrates the respective kinematics of the test rig, where:  $\alpha$  – pitch angle (indicated by the tested sensor),  $\gamma$  – roll angle,  $\eta$  – complement of angle  $\beta$  (indicated indirectly by the tested sensor – see Eq. (2)) as proposed by the author et al in [12],  $g$  – gravitational acceleration,  $g_x$ ,  $g_y$ ,  $g_z$  – Cartesian components of the acceleration  $g$ . The coordination system  $x_0y_0z_0$  is immovable, and the axis  $z_0$  overlaps direction of the gravitational acceleration. The coordination system  $xyz$  is attached to the tested tilt sensor. At the initial position axes of both systems overlap each other.

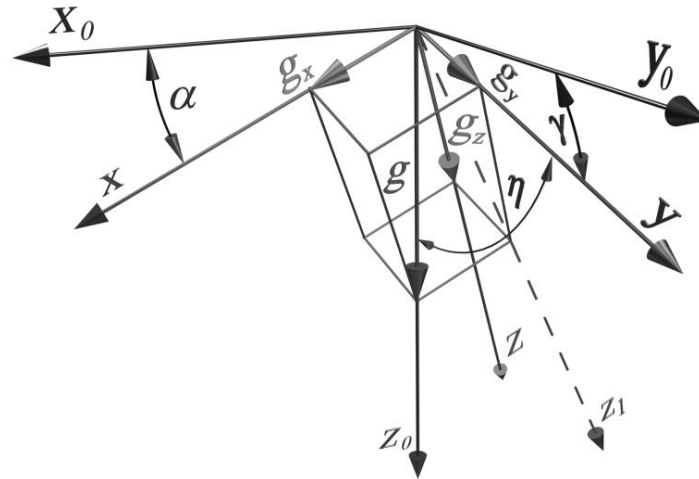


Fig. 1. Tilt angles applied by means of the test rig.

Operation of the test rig can be described as follows. A chosen angular position is approached in two steps. First, the tested sensor is turned around the horizontal axis  $y_0$ , and thus a pitch angle  $\alpha$  is applied. As a result, positions of axis  $x$  and  $z$  change. The later will be located in an intermediate position designated as  $z_I$ . Axis  $y$  still overlaps axis  $y_0$ . The respective output signal of the tested sensor changes then according to the following formula:

$$g_x = g \cdot \sin \alpha. \tag{1}$$

Subsequently, the sensor is turned around the axis  $x$  and in this way a roll angle  $\gamma$  is applied. As a result, axis  $y$  relocates from position  $y_0$  and axis  $z$  from the intermediate position  $z_I$ . Since the rotation took place around axis  $x$ , the output signal related to this axis does not change, whereas the second output signal of the tested sensor can be determined as follows:

$$g_y = g \cdot \cos \eta = g \cdot \sin \beta. \tag{2}$$

It should be noted that axis  $y$  and  $y_0$  create a plane  $yy_0$  tilted by angle  $\alpha$  with respect to the vertical, i.e. axis  $z_0$ . Therefore, the acceleration component on axis  $y$  (determined by angle  $\beta$ ) will be dependent both on angle  $\alpha$  as well as  $\gamma$  – it is explained in Fig. 2, which justifies the following formula:

$$g_y = g_\alpha \cdot \sin \gamma = g \cdot \cos \alpha \cdot \sin \gamma. \tag{3}$$

By combining Eq. (2) with (3) we can obtain a relation between angle  $\beta$  (indicated indirectly by the tested sensor) and pitch  $\alpha$  and roll  $\gamma$  applied by means of the test rig:

$$\beta = \arcsin(\sin \gamma \cdot \cos \alpha). \tag{4}$$

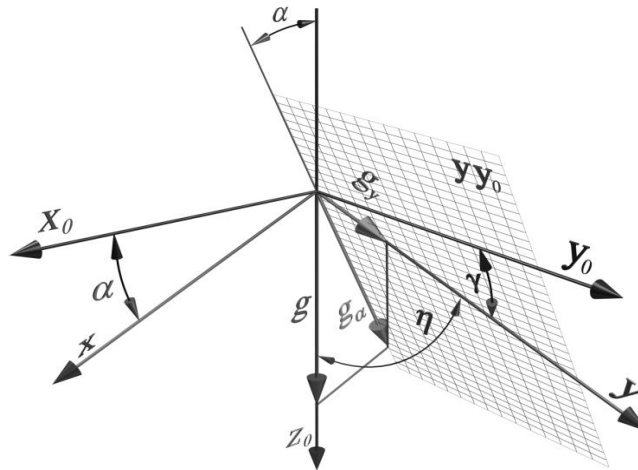


Fig. 2. The components of the gravity vector against pitch  $\alpha$  and roll  $\gamma$ .

### 3. The test rig

The test rig, schematically shown in Fig. 3, consists of four modules, which are:

- a computer system with an analog-digital data acquisition card operating under Windows system and running a custom software that controls the test rig,
- an electronic counter co-operating with an incremental angle encoder attached to the mechanical structure,
- a mechanical structure consisting basically of two rotation stages,
- an electronic module containing drivers of stepper motors and logics controlling the drivers.

The test rig operates in the following way. The software communicates with the electronic module via the analog-digital data acquisition card. Next, the electronic module actuates the mechanical structure (along with the tested sensor), applying a desired angular position of the rotation stages. Then, the analog output signals from the tested sensor are collected by the data acquisition card and recorded in a file against the corresponding real angular positions of the rotation stages.

Comparison of these two sets of data in a further processing is one of the ways of evaluating accuracy of the tested sensor.

The mechanical structure is constituted mainly by two rotation stages powered by stepper motors driving their tops through a worm gear. Nominal resolution of the rotation stages is of  $0.02^\circ$ . The stationary rotation stage is coupled with the angle encoder and applies pitch angle  $\alpha$ , while the movable rotation stage applies roll angle  $\gamma$ . The encoder is not necessary for a correct operation of the test rig, and should be regarded an enhancement increasing only accuracy of applying pitch angle.

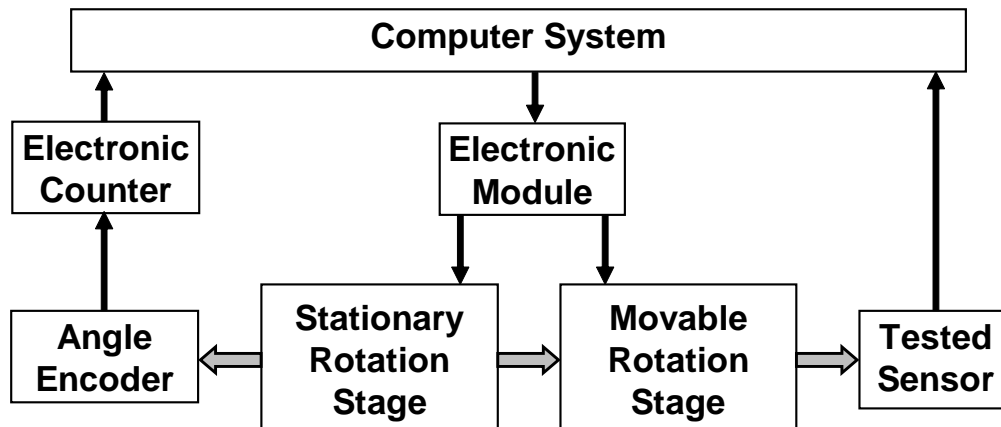


Fig. 3. Schematic of the test rig.

The tested tilt sensor can be fixed to the top of the movable rotation stage with application of a special aligning device presented in Fig. 4, which consists of three adjusting screws that while turned displace (within a small angular range) the tested sensor about  $x$ -,  $y$ - and  $z$ -axis, respectively (the arrows indicate direction of the displacement if the screws are turned clockwise). A triaxial angular displacement is possible owing to a compliant necking, which serves as an elastic bearing.

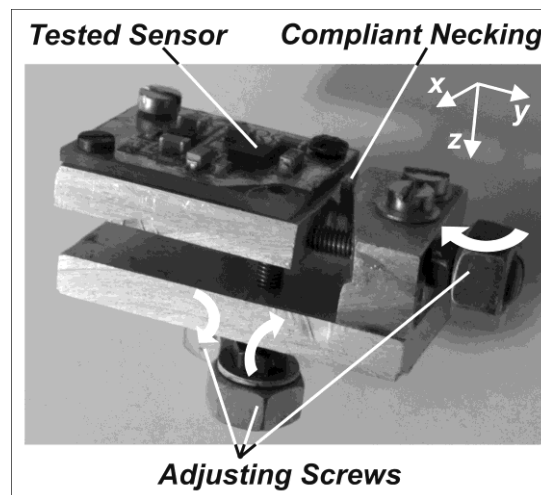


Fig. 4. Device for aligning and holding the tested sensors.

The issue of aligning the tested MEMS accelerometers is very significant, as proved by the author in [13]. Another approach to this problem is numerical compensation for the existing misalignments, proposed e.g. by Dias Pereira et al in [14].

#### 4. Accuracy of the test rig

The accuracy of the test rig is related to two issues:

- accuracy of reading the output analog voltages of the tested sensor,
- accuracy of applying angular position (pitch and roll) of the tested sensor.

In order to stick to the recommendations of ISO [15], a notion of uncertainty should be used rather than accuracy, which has a more general character. So, the following procedure

has been accepted:

- systematic errors (characteristic for operation of the rotation stages) were compensated for,
- the accuracies declared by the manufacturers of the used equipment were accepted as half-width of the intervals, within which the respective error can be always found,
- having no better information, it was assumed that it is equally probable that the error can be found in any part of the interval – so, a uniform distribution of possible values was assumed, as suggested by ISO in [15],
- the combined uncertainty was determined as the geometric sum of the component standard uncertainties (see Eq. (5) as an example),
- the expanded uncertainty was determined at the confidence level  $p = 99\%$  (for the respective coverage factor  $k_p$  of 1.71 [15]).

#### ***4.1. Uncertainty related to the data acquisition card***

The accuracy of measuring the analog output voltage of the tested sensor results from parameters of the applied data acquisition card, in this case Advantech PCI 1716. According to [16], the relevant parameters are as follows:

- resolution of the A/C converters: 16 bits,
- accuracy of reading the input voltage: 0.03% of the full scale range  $\pm 1$  bit (i.e. 1/65536) of this range.

Following the accepted procedure regarding the accuracy and using the above data, the extended combined uncertainty of measuring the input voltage  $U$  can be evaluated. For the widest range of the measured voltages that was used (i.e. 0 – 5 V), value of the expanded combined uncertainty will equal  $u(U) = 0.0015$  V. Since analog output signals of MEMS accelerometers contain usually a considerable offset, it is worthwhile to use the differential inputs of the card along with a reference voltage of a value similar to the offset. As proven by experimental tests, a reference voltage available at one of the outputs of some accelerometers (e.g. by MEMSIC Inc.) is noisy and thus cannot be employed for this purpose. However, the supply voltage of the accelerometers can be considered. Nevertheless, it must not be overlooked that a smallest possible range of the input voltages of the card should be used, e.g. 0 – 5 V or  $\pm 0.675$  V while using a reference voltage removing the offset.

#### ***4.2. Uncertainty related to the rotation stage***

In order to evaluate uncertainty of both rotation stages, appropriate tests have been carried out. Their angular displacements were calculated on the basis of the number of the steps performed at the nominal resolution of  $0.02^\circ$ , and at the same time measured by means of the incremental angle encoder IDW 2/16384 connected with the electronic counter AE 101 and coupled with the tested rotation stages by means of a precise coupling – all manufactured by Jenoptik Carl Zeiss JENA GmbH. The respective configuration was the same as in Fig. 3 with regard to the stationary rotation stage. Positioning error of the stages was defined as a difference between the calculated and measured displacement.

Accuracy of the angle encoder, as well as accuracy of the flexible coupling used is declared to be of 1 second arc [17]. Thus, applying the procedure accepted above, the combined expanded uncertainty of testing the rotation stages can be evaluated at  $0.0004^\circ$ .

Since the angle encoder is coupled with the stationary rotation stage during a standard operation of the test rig, so uncertainty of applying pitch is also of  $0.0004^\circ$ .

In order to evaluate uncertainty of the rotation stages, their positioning errors have been measured few times over one revolution. The uncertainty was determined on the basis of the

interval containing all the positioning errors.

In the case of using only one direction of rotation, width of the interval related to the movable rotation stage was of  $0.06^\circ$ . In the case of the stationary rotation stage, it has reached a value of  $0.08^\circ$ .

Since courses of the kinematic errors of the rotation stages contained a systematic component, it was possible to compensate for it. Then, the extended uncertainty has been determined as  $u(\gamma) = 0.02^\circ$  and  $u(\alpha) = 0.01^\circ$

### 4.3. Uncertainty related to pitch and roll

The test rig makes it possible to apply an arbitrary angular position (represented by pitch and roll) over the entire range of indications of the tested tilt sensor with a constant uncertainty resulted from uncertainty related to the rotation stages and the angle encoder.

However, in order to verify accuracy of tested sensors, angles  $\alpha$  and  $\beta$  must be first calculated using rearranged Eq. (1) and (2), or a more complicated dependency, like Eq. (9) introduced later in the text. Then, they must be compared with the pitch and the roll applied by means of the rotation stages. In the case of angle  $\alpha$  this can be accomplished directly, so the respective uncertainty results from uncertainty related to the angle encoder (or the stationary rotation stage). Yet, in the case of angle  $\beta$ , the applied pitch and roll angles must be combined on the basis of Eq. (4). This results in a variable uncertainty of determining the applied angle  $\beta$ .

A combined standard uncertainty of applying roll is to be estimated with the following formula, according to the guidelines of ISO [15]:

$$u_c(\beta) = \sqrt{\left(\frac{\partial\beta}{\partial\alpha} u(\alpha)\right)^2 + \left(\frac{\partial\beta}{\partial\gamma} u(\gamma)\right)^2}, \quad (5)$$

where:  $u_c(\beta)$  is combined uncertainty of angle  $\beta$ ;  $u(\alpha)$ ,  $u(\gamma)$  – standard uncertainty related to operation of the respective rotation stage;  $\alpha$  - pitch;  $\gamma$  - roll.

By substituting Eq. (4) to (5), and regarding the fact that:

$$u(\gamma) = 2u(\alpha), \quad (6)$$

we obtain the following equation:

$$u_c(\beta) = u(\gamma) \sqrt{\frac{\cos^2 \alpha \cdot \cos^2 \gamma + 0.25 \sin^2 \alpha \cdot \sin^2 \gamma}{1 - \cos^2 \alpha \cdot \sin^2 \gamma}}. \quad (7)$$

The maximal value of Eq. (7) over the full domain of angles  $\alpha$  and  $\gamma$  equals the uncertainty related to operation of the moveable rotation stage  $u(\gamma)$ . In all the other cases it is lower. Therefore, it can be stated that computing angle  $\beta$  according to Eq. (4) does not result



in increase of the respective uncertainty, and the combined uncertainty can be finally accepted as  $u_c(\beta)_{\max} = u(\gamma) = 0.02^\circ$ . The same applies to the case, when the angle encoder is used.

## 5. Experimental studies

Experiments performed using the described test rig allow metrological parameters of the tested sensor to be determined and verified.

Before starting the experiments (that should be performed at a constant ambient temperature and supply voltage, with no external vibration present, and having a knowledge of instantaneous, or approximate value of the gravitational acceleration), it is crucial to properly fix the tested sensor in the test rig, aligning its sensitive axes with the respective rotation axes of the test rig [18]-[19]. In this process, the holder presented in Fig. 4 is very useful. (Another interesting approach, which eliminates the laborious aligning process, has been proposed e.g. by Qian et al in [7] and Parsa et al in [20], where the misalignment errors of a roughly aligned accelerometer had been included in respective matrix equations, and then their values were estimated on the basis of statistical processing of the experimental data. However, it is hard to evaluate effectiveness of such approach in the terms of the resultant accuracy.)

Fig. 5 illustrates indication errors of a tested tilt sensor built of two MEMS accelerometers ADXL 202E manufactured by Analog Devices Inc., oriented perpendicularly to each other (thus measuring the three Cartesian components of the gravitational acceleration). The accuracy of the sensor can be evaluated with the error expressed over axis  $y$ , which has been defined by the author et al in [12] as follows:

$$e = |\beta - \phi|, \quad (8)$$

where:  $\beta$  is the roll angle indirectly applied by means of the test rig, and  $\phi$  is the roll angle that results from computing an average of respective indications of the tested sensor, (measured by means of the data acquisition card) according to an arc tangent-type of function (just as in the case of a robot presented in [21]), as proposed in [22]:

$$\phi = \arctg \frac{g_y}{\sqrt{g_x^2 + g_z^2}}. \quad (9)$$

In order to implement Eq. (9), signals of the tested accelerometers related to each sensitive axis had been appropriately calibrated using the presented test rig. Thus, individual values of the respective offsets and gains were determined and then employed while computing the component gravity accelerations.



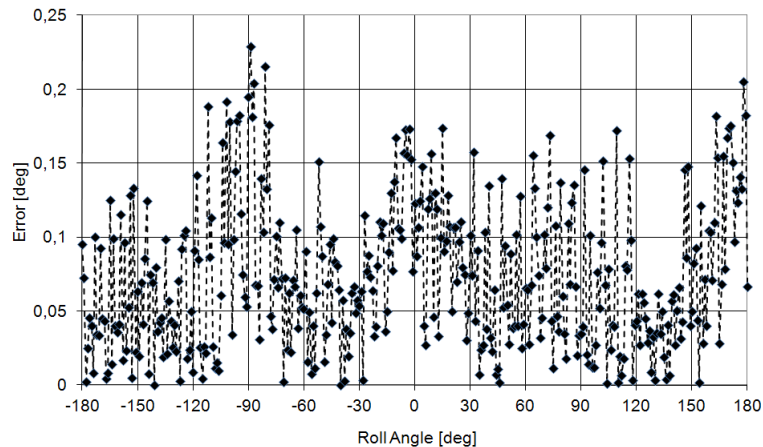


Fig. 5. Exemplary results of the experimental studies.

As can be observed, the error of determining the roll did not exceed  $0.23^\circ$  and had a similar course within the whole range of the roll, owing to application of arc tangent-type Eq. (9). With regard to the respective catalog datasheet [23], error of the accelerometer indications resulting only from the noise would exceed  $0.3^\circ$ , while the declared cross-axis sensitivity would increase it by another  $1.8^\circ$ .

## 6. Conclusions

The presented dual-axis test rig can be characterized by the following features:

- the analog output voltage of a tested sensor measured with uncertainty of  $0.0015\text{ V}$  within the range of  $0 - 5\text{ V}$ ,
- roll applied with uncertainty of  $0.02^\circ$  over  $360^\circ$  at the confidence level of 99%,
- angle  $\beta$  (indicated indirectly by accelerometer) determined with uncertainty of  $0.02^\circ$  over  $360^\circ$  at the confidence level of 99%,
- pitch applied with uncertainty of  $0.0004^\circ$  over  $360^\circ$  (or  $0.01^\circ$  in a configuration without the angle encoder) at the confidence level of 99%.

Such uncertainties are low enough for testing tilt sensors based on MEMS accelerometers.

Results of the performed tests revealed that the evaluated uncertainty of the tested accelerometers was much better, compare to the one reported in the respective catalog data. The same concerns the value of their cross-axis sensitivity, what was observed by other researchers too, e.g. by Acar and Shkel in [4].

In light of the above, it can be stated that performing experimental studies of MEMS accelerometers, provided an appropriate methodology and test rig are applied, is one of the most effective ways of improving their performance. Such approach has been employed not only in research practice, but also implemented commercially, e.g. in the case of a triaxial accelerometer module presented in [24], where individual testing of each component sensor made it possible to compensate for the offset, gain, cross-axis sensitivity and misalignment of each sensitive axis, and thus accuracy of the module has been significantly improved. However, its price is much higher compare to the employed accelerometers.

The described test rig can be also used for studying other metrological parameters of tilt sensors, not referred to in the paper, like inherent misalignment of their sensitive axes, linearity of the output signals and change of the performance characteristic due to ageing – see Tab. 1.

Even though the presented test rig features many advantages, there are of course some limitations related to its application. It cannot provide a controllable variable acceleration source, so dynamic properties of the tested sensors cannot be determined, except for studies of their pulse response. Due to vibration generated by the rotation stages (powered by stepping motors), hysteresis of the tested sensors cannot be estimated either, even though the incremental angle encoder ensures a satisfactory accuracy (rotation stage not coupled with an encoder is not accurate enough in this case). Therefore, a device manually driven would be a preferable solution here. The test rig is irrelevant with respect to MEMS accelerometers with measuring range exceeding few  $g$  because of using the gravitational acceleration as the reference.

Table 1. Scope of application of the test rig.

Tested Parameter	Fitness of the Test Rig	Angle Encoder Necessary	Remarks
<b>MEMS Accelerometers/Tilt Sensors</b>			
Gain	YES	NO	Also its uncertainty
Offset	YES	NO	Also its uncertainty
Uncertainty	YES	NO	
Linearity	YES	NO	
R-squared coefficient	YES	NO	
External misalignment	YES	NO	Referenced to some geometrical datum
Inherent misalignment	YES	YES	Referenced to other sensitive axes; does not apply to single-axis devices
Cross-axis sensitivity	YES	NO	
Pulse response	YES	NO	External or internal excitation
Mechanical hysteresis	NO	YES	No vibration allowed; small axial plays required
Dynamic parameters	NO	YES	Variable reference source required
<b>Tilt sensors</b>			
Error of tilt indications	YES	NO	Determined e.g. according to Eq. (9)
Error of tilt indications over a low-range	YES	YES	Precise tilt sensors

Parameters listed in the first part of Tab. 1 (MEMS Accelerometers/Tilt Sensors) are related to particular sensitive axis and refer both to accelerometers themselves as well as to tilt sensors (including solutions not based on accelerometers), accordingly. The first 5 parameters listed can be determined by performing a single calibration process, where successive tilt angles (either pitch or roll) are applied by means of the test rig, and the output signals of the tested sensor are recorded.

Concluding, few ways of improving performance of the test rig can be proposed here:

- a more accurate data acquisition card can be applied (e.g. PCI-1741 by Advantech Inc.),
- reference voltage should be introduced, as discussed in sec. 4.1 – the respective uncertainty of reading the measured output voltages would be then of 0.0012 V,
- in the case of applying only the pitch angle, the tested sensor can be attached to the output shaft of the angle encoder, providing thus much more stable position of its rotation axis (the stationary rotation stage is then used only as a drive); additionally, a special coupling between the rotation stage and the angle encoder can be employed then for damping the generated vibration.

On the contrary, when low cost of the test rig is pursued, the expensive angle encoder can be eliminated – such configuration is satisfactory e.g. while calibrating low-range MEMS accelerometers – see Tab. 1. Besides, if the tested MEMS accelerometers generate digital output signals (what usually results in their lower accuracy), the data acquisition card can be also eliminated. Then, one can obtain a test rig that is radically more cost-effective compare to expensive sophisticated solutions, which are usually applied in experimental works, like e.g. the measurement system presented e.g. in [25].

### Acknowledgments

The author would like to thank a graduate of the Faculty of Mechatronics, Warsaw University of Technology – Mr. Łukasz Kozłowski, M.Sc. Eng. for designing and building a prototype of the aligning device presented in Fig. 4.

### References

- [1] Bütefisch, S., Schoft, A., Büttgenbach, S. (2000). Three-Axes Monolithic Silicon Low-g Accelerometer. *J. Microelectromech. Syst.*, 9(4), 551–556.
- [2] Šipoš, M., Pačes, P., Roháč, J., Nováček, P. (2012). Analyses of triaxial accelerometer calibration algorithms. *IEEE Sensors J.*, 12(5), 1157–1165.
- [3] Frosio, I., Pedersini, F., Borghese, N.A. (2012). Autocalibration of Triaxial MEMS Accelerometers With Automatic Sensor Model Selection. *IEEE Sensors J.*, 12(6), 2100–2108.
- [4] Acar, C., Shkel, A. (2003). Experimental evaluation and comparative analysis of commercial variable-capacitance MEMS accelerometers. *J. Micromech. and Microeng.*, 13(5), 634–645.
- [5] Won, S.P., Golnaraghi, F. (2010). A Triaxial Accelerometer Calibration Method Using a Mathematical Model. *IEEE Trans. Instr. Meas.*, 59(8), 2144–2153.
- [6] Yun, S.S., Jeong, D.H., Wang, S.M., Je, C.H., Lee, M.L., Hwang, G., Choi, C.A., Lee, J.H. (2009). Fabrication of morphological defect-free vertical electrodes using a (1 1 0) silicon-on-patterned-insulator process for micromachined capacitive inclinometers. *J. Micromech. Microeng.*, (19), 035025.
- [7] Qian, J., Fang, B., Yang, W., Luan, X., Nan, H. (2011). Accurate Tilt Sensing with Linear Model. *IEEE Sensors J.*, 11(10), 2301–2309.
- [8] Ang, W.T., Khosla, P.K., Riviere, C.N. (2007). Nonlinear regression model of a low-g MEMS accelerometer. *IEEE Sensors J.*, 7(1), 81–88.
- [9] Latt, W.T., Veluvolu, K.C., Ang, W.T. (2011). Drift-Free Position Estimation of Periodic or Quasi-Periodic Motion using Inertial Sensors. *Sensors*, 11(6), 5931–5951.
- [10] Kibrick, R., Robinson, L., Cowley, D. (1995). An evaluation of precision tilt-sensors for measuring telescope position. In *Proc. Telescope Contr. Syst., SPIE Symposium on OE/Aerosp. Sensing and Dual Use Photon.*, Orlando, FL, USA, 364–376.
- [11] Popowski, S. (2008). Determining Pitch and Roll in Inexpensive Land Navigation Systems. *J. Aeronautica Integra*, 1(3), 93–97.

- [12] Łuczak, S., Oleksiuk, W., Bodnicki, M. (2006). Sensing Tilt with MEMS Accelerometers. *IEEE Sensors J.*, 6(6), 1669–1675.
- [13] Łuczak, S. (2013). Effects of Misalignments of MEMS Accelerometers in Tilt Measurements. In Brezina, T., Jabłoński, R. (Eds). *Mechatronics 2013. Recent Technological and Scientific Advances*, Berlin Heidelberg: Springer-Verlag, 393–400.
- [14] Dias Pereira, J.M., Viegas, V., Postolache, O., Girão, P.S. (2013). A smart and distributed measurement system to acquire and analyze mechanical motion parameters. *Metrol. Meas. Syst.*, 20(3), 465–47.
- [15] European co-operation for Accreditation (1999). *Expression of the Uncertainty of Measurement in Calibration*. EA-4/02. Geneva: International Organization for Standardization.
- [16] Advantech Co., Ltd. (2007). PCI-1716/1716 L 16-bit, 250 kS/s High-Resolution Multifunction Card. Startup Manual.
- [17] Jenoptik Carl Zeiss JENA GmbH (1989). IDW Incremental Transillumination Angle-Measuring System.
- [18] Chen, H., Bao, M., Zhu, H., Shen, S. (1997). A piezoresistive accelerometer with a novel vertical beam structure. *Sensors & Actuators, A* 63, 19–25.
- [19] MEMSIC Inc. (2005). Low g Accelerometer Non-Linearity Measurement. AN-00MX-014 Application Note n/r 5/12/03.
- [20] Parsa, K., Lasky, T.A., Ravani, B. (2007). Design and Implementation of a Mechatronic, All-Accelerometer Inertial Measurement Unit. *IEEE/ASME Trans. Mechatr.*, 12(6), 640–650.
- [21] Liu, Y., Liu, G. (2009). Track–Stair Interaction Analysis and Online Tipover Prediction for a Self-Reconfigurable Tracked Mobile Robot Climbing Stairs, *IEEE/ASME Trans. Mechatr.*, 14(5), 528–538.
- [22] Łuczak, S. (2007). Advanced Algorithm for Measuring Tilt with MEMS Accelerometers. In Jablonski, R., Turkowski, M. and Szewczyk, R. (Eds). *Recent Advances in Mechatronics*, Berlin Heidelberg: Springer-Verlag, 511–515.
- [23] Analog Devices Inc. (2000). Low Cost  $\pm 2g$  Dual Axis Accelerometer with Duty Cycle Output, ADXL 202E.
- [24] Sentra Technology Corporation (2003). AX301 Three-Axis Accelerometer Module, Preliminary Specifications.
- [25] Wengierow, M., Sałbut, L., Ramotowski, Z., Szumski, R., Szykiedans, K. (2013). Measurement System Based on Multi-Wavelength Interferometry for Long Gauge Block Calibration. *Metrol. Meas. Syst.*, 20(3), 479–490.